

Exact results for the two-dimensional Ising model in a magnetic field: Tests of finite-size scaling theory

Borko Stošić

*Laboratory for Solid State Physics and Radiation Chemistry, Boris Kidric Institute, Vinca,
P.O. Box 522, YU-11001 Belgrade, Yugoslavia*

Sava Milošević

Faculty of Physics, University of Belgrade, P.O. Box 550, YU-11001 Belgrade, Yugoslavia

H. Eugene Stanley

Center for Polymer Studies and Department of Physics, Boston University, Boston, Massachusetts 02215

(Received 13 October 1989; revised manuscript received 31 January 1990)

We use the transfer-matrix method to calculate density-of-states (DOS) functions for fully finite Ising-model systems. In this way, we obtain expressions for the corresponding partition functions for systems of sizes up to 12×12 in zero field and up to 8×8 in nonzero external magnetic field. We also establish a way of representing the DOS functions, in terms of the suitably scaled variables, that reveals a remarkably rapid convergence of these functions towards their thermodynamic limiting values as the system size increases. This rapid convergence implies that results obtained for systems of small sizes contain a surprisingly large amount of information about the behavior of infinite systems. In particular, we demonstrate that the finite-size-scaling-theory predictions are satisfied for small systems (treated exactly via this method) comparably well as for much larger systems (treated approximately via the Monte Carlo method). In addition, applying the method to the square Ising model in a nonzero field, we discover that the DOS functions for small systems display a regularity that one would expect to appear only for very large systems.

I. INTRODUCTION

The statistics of the two-dimensional (2D) Ising model in zero field is considered to be exactly known. However, there are still many questions that remain to be answered, in particular in the case of finite-size systems. The exact solution is well known¹⁻³ for periodic boundary conditions (PBC's), but the solution for systems of arbitrary size and shape with free boundary conditions (FBC's) is still unknown. In more complicated cases (nonzero homogeneous field, random impurities, random field, etc.), despite the fact that much useful information has been obtained by various techniques, there are generally no exact closed-form solutions.

In this paper we use the transfer-matrix method to find the partition function of fully finite-size systems, by calculating explicitly sets of all possible energy levels and the corresponding degeneracies. We demonstrate that in each particular case there is a rapid convergence of the density-of-states (DOS) functions for systems of increasing sizes, towards their thermodynamic limiting values. Surprisingly, this convergence sets in for very small systems and its behavior provides means to learn thermodynamics of the infinite system.

There were attempts to study the DOS functions in the past,^{4,5} but the rapid convergence of these functions was not observed. In the case of the Ising model on the square lattice, two decades ago Ono *et al.*⁴ and Suzuki *et al.*⁵ calculated the DOS functions of the systems up to sizes 5×5 for zero field ($H=0$) and nonzero field, spec-

tively. A straightforward application of their method^{4,5} of calculating the DOS functions using the most powerful present-day computers would provide results for systems up to sizes 7×7 . In this paper we use the transfer-matrix method^{6,7} to calculate the DOS functions for much larger systems. We have obtained results for systems of sizes up to 8×8 in the $H \neq 0$ case and 12×12 for $H=0$.⁸ It should be emphasized that by using this method on a present-day supercomputer one could obtain results for systems up to sizes 16×16 . Finally, it should be observed that the idea of utilizing the DOS function for learning the thermodynamics of a system is quite similar to the recently suggested method⁹ of using a single Monte Carlo simulation to obtain complete thermodynamic information near a phase transition. In fact, the suggested new Monte Carlo method⁹ is based on a single *estimate* of the DOS function weighted by corresponding Boltzmann factors at a chosen temperature and field.

The rapid convergence of the DOS functions that we have observed sheds new light on the finite-size scaling of the thermodynamic response functions. For instance, in the Monte Carlo approach to testing finite-size scaling (Landau^{10,11}), the presentation of results is obscured by both the small size of the systems studied and the statistical error inherent of the Monte Carlo technique. Our exact data for specific heat and susceptibility calculated from the DOS functions show a surprisingly regular collapsing tendency even in the critical region pertinent to the infinite system (although the systems we have studied are much smaller than those treated by Landau^{10,11}).

This fact implies, contrary to the general belief, that very small systems contain a considerable amount of information about the limiting behavior of the infinite system in the critical region. It thus follows that it is more important, in the case of approximate studies of finite-size systems, to reduce the error germane to the method applied, than to increase the system size.

The structure of this paper is as follows. In Sec. II we give the general description of the transfer-matrix method of calculating the DOS functions. We also elaborate a specific way of presenting the DOS functions that yields convergence of the data for systems of different sizes, and illustrate it in the case of the 1D Ising model. In Sec. III we apply these ideas to the FBC's Ising model case, in a zero field, on the square and triangular lattice, whereas the $H \neq 0$ case on the square lattice we treat in Sec. IV. Finally, in Sec. V we discuss the obtained results and their implications.

II. CALCULATING AND REPRESENTING THE DOS FUNCTIONS

A. Transfer-matrix method for calculating the DOS functions

In what follows we discuss the transfer-matrix (TM) method in the case of a 2D homogeneous Ising model with nearest-neighbor (NN) interactions, in a zero field. The basic idea of the TM method^{6,7} consists of conceiving a system of $n \times m$ Ising spins as a set of m mutually interacting chains of n spins. Each of the chains has 2^n possible configurations labelled by γ ($\gamma = 1, 2, \dots, 2^n$). If the spins of the last chain are fixed in one particular configuration γ , summation over all the possible configurations of all the other spins produces the corresponding partial partition function $Z^{(m)}(\gamma)$ (in order to simplify notation, we have omitted here the index n , which denotes the width of the system; such collapsing of notation will be applied wherever it does not cause ambiguities). The total partition function is given by

$$Z^{(m)} = \sum_{\gamma=1}^{2^n} Z^{(m)}(\gamma). \quad (1a)$$

If the system is now increased by adding one new ($m=1$)-th chain, the recursive relation for the partial partition functions is

$$Z^{(m+1)}(\gamma') = \sum_{\gamma=1}^{2^n} Z^{(m)}(\gamma) e^{-\beta[E(\gamma') + E_{\text{int}}(\gamma, \gamma')]} \quad (1b)$$

Here β is the reciprocal of the product of the Boltzmann constant k_B and temperature T and $E(\gamma')$ is the energy of the added chain in configuration γ' , with $E_{\text{int}}(\gamma, \gamma')$ being the interaction energy of the last two chains.

From this point one may proceed to calculate the set $Z^{(1)}(\gamma)$, $\gamma = 1, 2, \dots, 2^n$, for a single chain, and using (1b) find the set $Z^{(m)}(\gamma)$. The partition function is then found using (1a). This is the usual procedure of the TM method.⁷ The power of this method lies in the fact that in order to find the partition function one needs to perform roughly speaking $m2^{2n}$ operations compared to

sweeping over 2^{nm} different spin configurations.^{4,5} The largest systems that have been studied using the TM method had $n = 18$ (see Ref. 7). One should observe that the direct calculation of the partition function of a system with 18×18 spins would require sweeping over $2^{324} \approx 3 \times 10^{97}$ configurations, which is far beyond any conceivable present-day computer power! On the other hand, the limitations of the TM method are set by memory requirements as well as CPU time. Also, a new computer run, in the TM case, has to be made for each given value of temperature and interaction strength.

The idea of the TM method may be pursued further⁶ by considering the sets of possible energy levels at each stage of the construction of the lattice, and the recursion relations for the corresponding degeneracies. At a given stage of construction the system has m chains of length n , with altogether $N_b^{(m)} = 2nm - n - m$ bonds. The ground-state energy level corresponds to the fully ordered spin configurations. All the excited states are obtained by upsetting k bonds ($0 < k \leq N_b^{(m)}$). A bond is considered to be upset, in the ferromagnetic case, if its end spins are antiparallel, whereas in the antiferromagnetic case the bond is upset if its end spins are parallel. Thus for the partition function one can write

$$Z^{(m)} = e^{\beta|J|N_b^{(m)}} \sum_{k=0}^{N_b^{(m)}} \mathcal{D}_k^{(m)} e^{-2k\beta|J|}. \quad (2a)$$

Here $|J|$ is the absolute value of the exchange energy of the nearest-neighbor spins, while $\mathcal{D}_k^{(m)}$ is the degeneracy of the energy level with k upset bonds

$$E_k^{(m)} = |J|(-N_b^{(m)} + 2k), \quad [k = 0, 1, 2, \dots, N_b^{(m)}]. \quad (2b)$$

Besides, since the total number of spin configurations is 2^{nm} , the following relation holds

$$\sum_{k=0}^{N_b^{(m)}} \mathcal{D}_k^{(m)} = 2^{nm}. \quad (2c)$$

For the partial partition functions the analog of (2a) is

$$Z^{(m)}(\gamma) = e^{\beta|J|N_b^{(m)}} \sum_{k=0}^{N_b^{(m)}} D_k^{(m)}(\gamma) e^{-2k\beta|J|}, \quad (3)$$

where $D_k^{(m)}(\gamma)$ are the corresponding degeneracies of energy levels (2b). If the system is increased by adding one new chain, the number of bonds becomes

$$N_b^{(m+1)} = 2n(m+1) - n - (m+1),$$

and the energy spectrum is given by the following analog of (2b):

$$E_k^{(m+1)} = |J|(-N_b^{(m+1)} + 2k'), \quad k' = 0, 1, 2, \dots, N_b^{(m+1)}. \quad (4)$$

For the increased system the partial partition functions have the form

$$Z^{(m+1)}(\gamma') = e^{\beta|J|N_b^{(m+1)}} \sum_{k'=0}^{N_b^{(m+1)}} D_k^{(m+1)}(\gamma') e^{-2k'\beta|J|}.$$

Inserting this formula and (3) into (1b) the recursion relations for the degeneracies are found to be

$$D_k^{(m+1)}(\gamma') = \sum_{\gamma=1}^{2^n} \sum_{k=0}^{N_b^{(m)}} D_k^{(m)}(\gamma) \delta(E_k^{(m+1)} - [E_k^{(m)} + E(\gamma') + E_{\text{int}}(\gamma, \gamma')]) , \quad (5a)$$

with

$$D_k^{(m)} = \sum_{\gamma=1}^{2^n} D_k^{(m)}(\gamma) . \quad (5b)$$

Here δ is the Kronecker δ function, $E(\gamma')$ is the energy of the new chain in configuration γ' , and $E_{\text{int}}(\gamma, \gamma')$ the interaction energy of the last two chains. It should be observed that the value of δ does not depend on the value and sign of the interaction strength J , but only on the particular combination of k , k' , γ and γ' . In other words, in analogy to (2b) and (4) one can write

$$E(\gamma') = |J| [-(n-1) + 2l_{\gamma'}] , \quad 0 \leq l_{\gamma'} \leq n-1 , \quad (6a)$$

$$E_{\text{int}}(\gamma, \gamma') = |J| (-N + 2j_{\gamma, \gamma'}) , \quad 0 \leq j_{\gamma, \gamma'} \leq n , \quad (6b)$$

where $l_{\gamma'}$ is the number of upset bonds in the added chain in configuration γ' , whereas $j_{\gamma, \gamma'}$ is the number of upset bonds connecting the last two chains in their configurations γ and γ' . Equations (6a) and (6b), together with (2b) and (4), imply the new form of (5a)

$$D_k^{(m+1)}(\gamma') = \sum_{\gamma=1}^{2^n} \sum_{k=0}^{N_b^{(m)}} D_k^{(m)}(\gamma) \delta(k' - k - l_{\gamma'} - j_{\gamma, \gamma'}) . \quad (7)$$

This formula was first derived by Binder⁶ in 1972.

Hence one may proceed to find the degeneracies of the initial system, that is of a single chain, then apply the recursion relation (7) m times, and finally apply (5b) to obtain the degeneracies of the full $n \times m$ system. In implementing this algorithm, it is useful to observe that when applying (7), for a given combination of γ and γ' , it is not necessary to scan all possible combinations of k and k' in order to see which of them give a nonzero contribution. Instead, for each particular set γ, γ' and k , the δ function in (7) should be used to find that value of k' for which the degeneracy $D_k^{(m+1)}(\gamma')$ is increased by the term $D_k^{(m)}(\gamma)$. In this way the total number of necessary operations is reduced roughly from

$$N_b^{(m)} N_b^{(m+1)} 2^{2n} \approx (nm)^2 2^{2n+2}$$

to

$$N_b^{(m)} 2^{2n} \approx nm 2^{2n+1}$$

Compared with the numerical TM approach, represented by the formulas in (1), this approach increases both the memory and CPU time requirements. Thus the size of the largest system that can be studied is reduced, roughly speaking from the linear size $n=18$ to the size $n=16$. However, within this approach a single computer run is sufficient to generate all necessary information for all temperatures and all possible values of the interaction

strength, which means that the resulting equation for the partition function is a closed-form expression containing at most $N_b + 1$ terms. This is a considerable advantage comparing with the numerical TM approach which provides the partition function only in a tabular form

B. Convergence of the DOS functions

Here we present the argumentation that reveals the convergence of the DOS functions for systems of increasing sizes, towards their thermodynamic limiting values. Let us study an Ising system with N spins on a lattice of arbitrary geometry, in a zero field. In analogy to (2) the partition function of the system is

$$Z^{(N)} = e^{\beta|J|N_b} \sum_{k=0}^{N_b} \mathcal{D}_k^{(N)} e^{-2k\beta|J|} , \quad (8a)$$

where N_b is the number of bonds, and $\mathcal{D}_k^{(N)}$ is the degeneracy of the energy level with k upset bonds

$$E_k^{(N)} = |J| (-N_b + 2k) , \quad k=0, 1, 2, \dots, N_b , \quad (8b)$$

and the sum of all degeneracies satisfies the condition

$$\sum_{k=0}^{N_b} \mathcal{D}_k^{(N)} = 2^N . \quad (8c)$$

In what follows it is convenient to introduce the dimensionless energy variable

$$\tilde{k} = (E_k^{(N)} - E_{\min}^{(N)}) / (E_{\max}^{(N)} - E_{\min}^{(N)}) = k / N_b , \quad (9)$$

where the minimum and the maximum energy levels are given by $E_{\min}^{(N)} = -|J|N_b$ and $E_{\max}^{(N)} = |J|N_b$, respectively. The new variable \tilde{k} takes values in the interval $0 \leq \tilde{k} \leq 1$, regardless of the size and shape of the system. At this moment we define the function $\mathcal{D}^{(N)}(x)$, of the continuous variable $x \in [0, 1]$, by the requirement that it interpolates the density of states function $\mathcal{D}_k^{(N)}$, which is itself defined at the points $x = \tilde{k} = 0, 1/N_b, 2/N_b, \dots, 1$. Of course, there is an infinite set of functions that satisfy the interpolation requirement, but here we suppose that we are dealing with one of the functions whose derivatives at each x follow local behavior of the set of values $\mathcal{D}_k^{(N)}$. The introduction of the function $\mathcal{D}^{(N)}(x)$ is necessary only for comparison of different discrete sets $\mathcal{D}_k^{(N)}$ (calculated for systems of different sizes), because the latter are, in general, determined for disjoint sets of points.

If the system is increased by adding one new spin in such a way that it interacts with the spins of the old system through s bonds, the analogs of (8) are given by

$$Z^{(N+1)} = e^{\beta|J|(N_b+s)} \sum_{k'=0}^{N_b+s} \mathcal{D}_{k'}^{(N+1)} e^{-2k'\beta|J|} , \quad (10a)$$

$$E_{k'}^{(N+1)} = |J| [-(N_b+s) + 2k'] , \quad k'=0, 1, 2, \dots, N_b+s , \quad (10b)$$

$$\sum_{k'=0}^{N_b+s} \mathcal{D}_{k'}^{(N+1)} = 2^{N+1} . \quad (10c)$$

It should be noticed that the energy spectrum is increased by s new levels, while the total number of spin configurations is doubled. Now we can compare the two DOS functions by defining the ratio

$$\alpha^{(N+1)}(x) = \mathcal{D}^{(N+1)}(x) / \mathcal{D}^{(N)}(x) . \tag{11}$$

For N so large that the variables \tilde{k} and \tilde{k}' can be considered effectively continuous, the quantity $\alpha^{(N)}(x)$ in fact describes the way the number of spin configurations with energies close to x changes when one new spin is added to the system. Furthermore, for large enough systems, when the boundary conditions can be neglected, we may expect that $\alpha^{(N)}(x)$ becomes independent of size of the systems. In other words, we assume that for any given accuracy of determining the DOS functions there exists a minimum number of spins M , such that

$$\alpha^{(N)}(x) = \alpha(x), \quad N > M . \tag{12}$$

Using (11) we proceed by writing

$$\mathcal{D}^{(N)}(x) = \prod_{i=1}^N \alpha^{(i)}(x) , \tag{13}$$

and from (12) we obtain

$$\mathcal{D}^{(N)}(x) = c(x) [\alpha(x)]^N , \tag{14a}$$

where

$$c(x) = \prod_{i=1}^M \alpha^{(i)}(x) / [\alpha(x)]^M . \tag{14b}$$

Thus it follows that the functions

$$\ln \mathcal{D}^{(N)}(x) / N = \ln c(x) / N + \ln \alpha(x) , \tag{15}$$

and the corresponding sets

$$\ln \mathcal{D}_k^{(N)} / N, \quad k = 0, 1, 2, \dots, N_b ,$$

should become independent of N for large systems. In other words, for sufficiently large systems we can expect convergence of the sets

$$\ln \mathcal{D}_k^{(N)} / N, \quad k = 0, 1, 2, \dots, N_b ,$$

when these sets are represented graphically as functions of the variable $\tilde{k} = k / N_b$. Rewriting (8a) as

$$\mathcal{Z}^{(N)} = e^{\beta |J| N_b} \sum_{k=0}^{N_b} \exp [N_b (- 2 \tilde{k} \beta |J| + \ln \mathcal{D}_k^{(N)} / N_b)] , \tag{16}$$

we see that for representing the DOS functions it is more convenient to use the sets $\ln \mathcal{D}_k^{(N)} / N_b$, which should also exhibit the above-mentioned convergence for large N , since $N_b / N \rightarrow \text{constant}$ when $N \rightarrow \infty$ for any given lattice. Namely, using these sets to compare the terms that appear in the expression (16) one can identify, for each given temperature and interaction strength, those energy levels and corresponding spin configurations that give the predominant contribution to the partition function. This fact will be demonstrated in the second part of the paper. Also, from the point of view of microcanonical ensemble,

the quantity $\ln \mathcal{D}_k^{(N)} / N_b$ may be regarded as the entropy per bond associated with the energy level E_k .

We will now illustrate how this approach of representing the DOS functions works in the simple case of the 1D Ising chain in zero field. The partition function of the chain of N spins with free boundary conditions ($N_b = N - 1$) is

$$\mathcal{Z}^{(N)} = 2^N \cosh^{N-1} (\beta |J|) . \tag{17}$$

Rewriting (17) in the form

$$\mathcal{Z}^{(N)} = 2 e^{(N-1)\beta |J|} (1 + e^{-2\beta |J|})^{N-1} , \tag{18}$$

we find

$$\mathcal{Z}^{(N)} = 2 e^{(N-1)\beta |J|} \sum_{k=0}^{N-1} \binom{N-1}{k} e^{-2k\beta |J|} . \tag{19}$$

Thus we see that the degeneracies $\mathcal{D}_k^{(N)}$ of the energy levels $E_k^{(N)} = -|J|(N-1-2k)$ are given by binomial coefficients $\binom{N-1}{k}$. In Fig. 1 we depict the sets

$$S^{(N)}(k) \equiv \ln \binom{N-1}{k} / (N-1)$$

versus variable $\tilde{k} = k / (N-1)$, where $k = 0, 1, 2, \dots, N-1$, for systems of sizes $N = 4, 8, 16, 32, 64, 128, 256$. In the limit $N \rightarrow \infty$ the variable $\tilde{k} \equiv x$ becomes continuous, and using Stirling formula we find

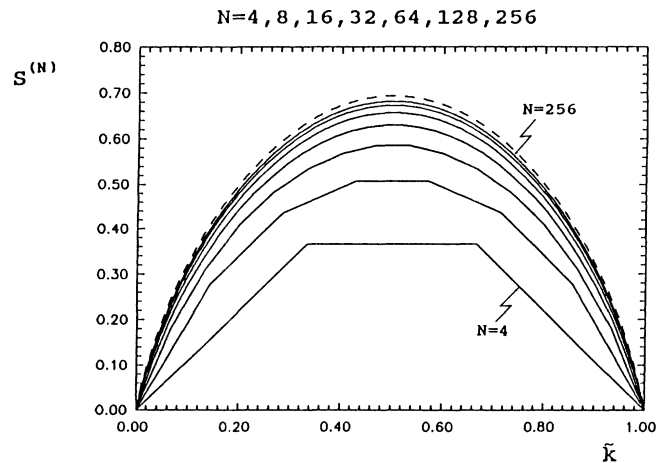


FIG. 1. The DOS functions of the Ising chain in zero field with $N = 4, 8, 16, 32, 64, 128, 256$ spins. The sets

$$S^{(N)}(k) \equiv \ln \binom{N-1}{k} / (N-1)$$

vs variable $\tilde{k} = k / (N-1)$ (where $k = 0, 1, 2, \dots, N-1$) are shown so that the individual points are connected with straight lines to guide the eye. The dashed curve represents the limiting DOS function $S(x)$ given by (20). One can observe a rather fast convergence of the finite-size system DOS functions towards the dashed curve which is pertinent to the infinite system ($N \rightarrow \infty$). This convergence of the DOS functions is more rapid in the case of the 2D Ising model.

$$S(x) = -x \ln x - (1-x) \ln(1-x). \quad (20)$$

From Fig. 1 we see that the sets $S(k)$ do exhibit the convergence towards the curve determined by (20), when the size of the spin system becomes ever increasing. We shall see later that this convergence of the DOS functions becomes more rapid in the 2D Ising model case.

III. CASE $d=2, H=0$

We first apply the above presented approach to the case of the Ising model on the square lattice with fully free boundaries. Thus we have calculated the DOS functions for the Ising systems with $n \times n$ spins, where $n=3, 4, \dots, 12$. Surprisingly, the obtained results are completely new, as the previously reported results^{4,5} were obtained up to $n=5$, and were pertinent to systems with periodic boundary conditions. Our results for $n=4, 5, 6$ are given in Table I. On the other hand, in Fig. 2 we plot the entropy $S^{(n)}(k) = \ln \mathcal{D}_k^{(n)} / N_b$ versus the scaled energy variable $\tilde{k} = k / N_b$ for all studied systems, that is for $n=3, 4, \dots, 12$. From this figure we can see that the corresponding curves for $n > 3$ merge into a bundle whose elements are hardly distinguishable, which vividly demonstrates the convergence discussed in the previous section. Such a behavior of the DOS functions could

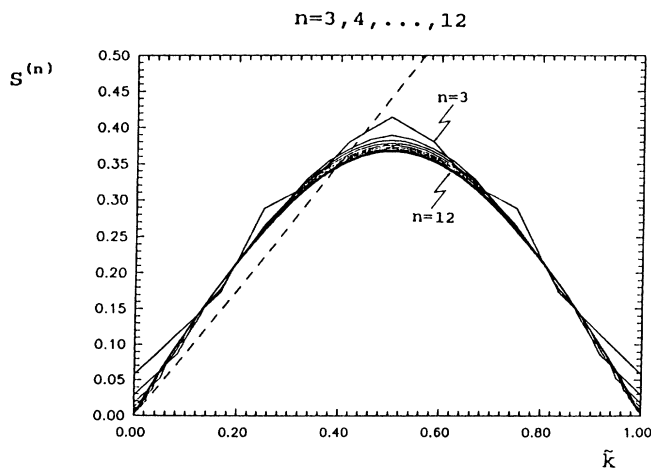


FIG. 2. The entropy per bond $S^{(n)}(k) = \ln \mathcal{D}_k^{(n)} / N_b$ vs the scaled energy variable $\tilde{k} = k / N_b$ for the square Ising model in zero field with $n \times n$ spins ($n=3, 4, \dots, 12$). The merging of the curves for $n > 3$ into a bundle whose elements are hardly distinguishable, demonstrates the rapid convergence of the DOS functions, with increasing system size, towards their thermodynamic limiting values. The dashed line has the slope $2\tilde{k}\beta_c J$ with $\beta_c J = \ln(1 + \sqrt{2})/2$ which corresponds to the critical temperature of the infinite system. The maximum difference between this line and the limiting curve, approximately represented by the $n=12$ curve, reveals the dominant contribution to the partition function at T_c . Thus we learn that at the critical temperature the spin configurations with roughly 80% of satisfied bonds give the dominant contribution to the partition function, and thereby to the thermodynamics of the system.

have been expected for very large n , and what comes as a surprise is the fact that it is observable already for $n > 3$. Consequently, it will appear that in applying the finite-size-scaling method,^{12,13} one may use information that comes from studying systems smaller than those used in the past.^{10,11}

In Sec. II we have observed that by comparing terms of the expression (16) one can identify, for each given temperature and interaction strength, those energy levels and corresponding spin configurations that give the predominant contribution to the partition function. Having the specific results presented in Fig. 2, it follows that for any given fixed value $\beta|J|$ one should draw a straight line with the slope $2\beta|J|$, and locate the maximum difference between this line and the limiting entropy curve. This difference and the pertinent value \tilde{k}_{\max} determine the maximum term in (16). It should be noticed that even those terms in (16) which correspond to values of \tilde{k} very close to \tilde{k}_{\max} , have much smaller contribution than the term with \tilde{k}_{\max} . This is due to the fact that all terms in (16) are in fact exponential functions of the differences $S - 2\tilde{k}\beta|J|$ multiplied by N_b , which is a large number. In Fig. 2 we draw the line $2\tilde{k}\beta_c J$ for $\beta_c J = \ln(1 + \sqrt{2})/2$, which corresponds to the critical temperature of the infinite system. Hence, if we suppose that the entropy curve for infinite system cannot depart much from the bundle of curves depicted in Fig. 2, one can infer that in the critical region the dominant energy levels are those which are associated with configurations consisting of roughly 80% satisfied bonds.

We have also performed calculations for the Ising sys-

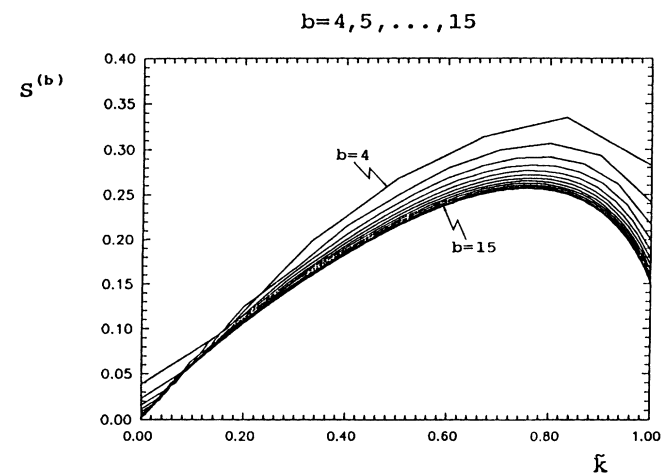


FIG. 3. The scaled DOS functions for the Ising model on the equilateral wedge of the triangular lattice with $b=4, 5, \dots, 15$ spins on a side, in zero field. The individual points are connected with straight lines to guide the eye. The convergence is less rapid than in the square lattice case (cf. Fig. 2), which can be attributed to the larger ratio of the number of spins on the edges vs the number of interior spins. The asymmetric form of the curves corresponds to the topological frustration of the Ising antiferromagnet on the triangular lattice at low temperatures.

TABLE I. The partition functions $Z^{(n)}$, $n=4,5,6$, of the fully finite ($n \times n$) square Ising system with free boundary conditions and in a zero field, represented according to formula (8a). One should observe that the line which would connect all the “exp” signs within each term of $Z^{(n)}$ would be, in fact, a representation of the DOS function curve $\mathcal{D}^{(n)}$ versus unscaled energy variable. Besides, one can see that the three such curves (for $n=4,5,6$) have notably different widths and heights. However, via a proper scaling (cf. Fig. 2), with increasing system size all these curves rapidly converge towards their thermodynamic limiting values. Finally, it should be mentioned that no expression for $Z^{(5)}$ and $Z^{(6)}$ has been reported in literature so far. The same is true for $Z^{(n)}$, with $n=7,8,9,10,11,12$, which are available from the authors upon request.

$Z^{(4)}=2\exp(24\beta J)$	$Z^{(5)}=2\exp(40\beta J)$	$Z^{(6)}=2\exp(60\beta J)$
+ 8exp(20βJ)	+ 8exp(36βJ)	+ 8exp(56βJ)
+ 32exp(18βJ)	+ 40exp(34βJ)	+ 48exp(54βJ)
+ 72exp(16βJ)	+ 78exp(32βJ)	+ 100exp(52βJ)
+ 224exp(14βJ)	+ 256exp(30βJ)	+ 288exp(50βJ)
+ 584exp(12βJ)	+ 884exp(28βJ)	+ 1132exp(48βJ)
+ 1216exp(10βJ)	+ 2312exp(26βJ)	+ 3168exp(46βJ)
+ 2638exp(8βJ)	+ 5962exp(24βJ)	+ 8824exp(44βJ)
+ 4928exp(6βJ)	+ 15 554exp(22βJ)	+ 25 744exp(42βJ)
+ 7344exp(4βJ)	+ 37 412exp(20βJ)	+ 71 064exp(40βJ)
+ 9984exp(2βJ)	+ 84 424exp(18βJ)	+ 186 624exp(38βJ)
+ 11 472exp(0βJ)	+ 180 616exp(16βJ)	+ 484 210exp(36βJ)
+ 9984exp(-2βJ)	+ 362 136exp(14βJ)	+ 1 214 336exp(34βJ)
+ 7344exp(-4βJ)	+ 672 908exp(12βJ)	+ 2 931 560exp(32βJ)
+ 4928exp(-6βJ)	+ 1 157 160exp(10βJ)	+ 6 853 760exp(30βJ)
+ 2638exp(-8βJ)	+ 1 837 876exp(8βJ)	+ 15 444 302exp(28βJ)
+ 1216exp(-10βJ)	+ 2 658 328exp(6βJ)	+ 33 435 520exp(26βJ)
+ 584exp(-12βJ)	+ 3 474 900exp(4βJ)	+ 69 487 240exp(24βJ)
+ 224exp(-14βJ)	+ 4 108 408exp(2βJ)	+ 138 380 976exp(22βJ)
+ 72exp(-16βJ)	+ 4 355 924exp(0βJ)	+ 263 185 168exp(20βJ)
+ 32exp(-18βJ)	+ 4 108 408exp(-2βJ)	+ 476 852 512exp(18βJ)
+ 8exp(-20βJ)	+ 3 474 900exp(-4βJ)	+ 821 190 292exp(16βJ)
+ 2exp(-24βJ)	+ 2 658 328exp(-6βJ)	+ 1 340 056 928exp(14βJ)
	+ 1 837 876exp(-8βJ)	+ 2 065 952 532exp(12βJ)
	+ 1 157 160exp(-10βJ)	+ 3 000 507 536exp(10βJ)
	+ 672 908exp(-12βJ)	+ 4 093 604 824exp(8βJ)
	+ 362 136exp(-14βJ)	+ 5 230 849 920exp(6βJ)
	+ 180 616exp(-16βJ)	+ 6 244 335 166exp(4βJ)
	+ 84 424exp(-18βJ)	+ 6 951 501 824exp(2βJ)
	+ 37 412exp(-20βJ)	+ 7 206 345 520exp(0βJ)
	+ 15 544exp(-22βJ)	+ 6 951 501 824exp(-2βJ)
	+ 5 962exp(-24βJ)	+ 6 244 335 166exp(-4βJ)
	+ 2312exp(-26βJ)	+ 5 230 849 920exp(-6βJ)
	+ 884exp(-28βJ)	+ 4 093 604 824exp(-8βJ)
	+ 256exp(-30βJ)	+ 3 000 507 536exp(-10βJ)
	+ 78exp(-32βJ)	+ 2 065 952 532exp(-12βJ)
	+ 40exp(-34βJ)	+ 1 340 056 928exp(-14βJ)
	+ 8exp(-36βJ)	+ 821 190 292exp(-16βJ)
	+ 2exp(-40βJ)	+ 476 852 512exp(-18βJ)
		+ 263 185 168exp(-20βJ)
		+ 138 380 976exp(-22βJ)
		+ 69 487 240exp(-24βJ)
		+ 33 435 520exp(-26βJ)
		+ 15 444 302exp(-28βJ)
		+ 6 853 760exp(-30βJ)
		+ 2 931 560exp(-32βJ)
		+ 1 214 336exp(-34βJ)
		+ 484 210exp(-36βJ)
		+ 186 624exp(-38βJ)
		+ 71 064exp(-40βJ)
		+ 25 744exp(-42βJ)
		+ 8824exp(-44βJ)
		+ 3168exp(-46βJ)
		+ 1132exp(-48βJ)

TABLE I. (Continued).

	+ 288exp(− 50βJ)
	+ 100exp(− 52βJ)
	+ 48exp(− 54βJ)
	+ 8exp(− 56βJ)
	+ 2exp(− 60βJ)

TABLE II. The partition functions $Z^{(b)}$, $b=9,10$ of the Ising system on the fully finite equilateral wedge of the triangular lattice, with free boundary conditions and in a zero field. Here one can make the same comment, concerning the representation of the DOS functions, as in the caption of Table I. The new point in this table, compared with the Table I, is the fact that the curves connecting the exp signs are asymmetric with respect to the center of the energy scale. This fact can be related to the residual entropy (Ref. 14) of the Ising antiferromagnet on the triangular lattice (see the text).

$Z^{(9)}=2\exp(108\beta J)$ + 6exp(104βJ) + 66exp(100βJ) + 284exp(96βJ) + 1524exp(92βJ) + 6816exp(88βJ) + 29 374exp(84βJ) + 121 722exp(80βJ) + 478 944exp(76βJ) + 1 823 924exp(72βJ) + 6 649 848exp(68βJ) + 23 348 880exp(64βJ) + 78 567 870exp(60βJ) + 253 527 624exp(56βJ) + 782 097 738exp(52βJ) + 2 302 568 918exp(48βJ) + 6 449 220 270exp(44βJ) + 17 132 714 196exp(40βJ) + 43 009 989 732exp(36βJ) + 101 618 632 900exp(32βJ) + 224 923 586 992exp(28βJ) + 463 948 349 952exp(24βJ) + 886 492 447 232exp(20βJ) + 1 558 302 256 512exp(16βJ) + 2 499 881 356 672exp(12βJ) + 3 625 589 506 560exp(8βJ) + 4 700 549 738 496exp(4βJ) + 5 374 295 023 616exp(0βJ) + 5 328 810 812 928exp(− 4βJ) + 4 486 979 323 136exp(− 8βJ) + 3 123 272 658 048exp(− 12βJ) + 1 735 088 988 704exp(− 16βJ) + 733 979 231 256exp(− 20βJ) + 221 791 575 960exp(− 24βJ) + 43 730 599 644exp(− 28βJ) + 4 859 988 896exp(− 32βJ) + 220 240 306exp(− 36βJ)	$Z^{(10)}=2\exp(135\beta J)$ + 6exp(131βJ) + 72exp(127βJ) + 322exp(123βJ) + 1806exp(119βJ) + 8514exp(115βJ) + 38 106exp(111βJ) + 165 732exp(107βJ) + 678 780exp(103βJ) + 2 718 084exp(99βJ) + 10 454 808exp(95βJ) + 39 101 634exp(91βJ) + 141 628 968exp(87βJ) + 497 491 620exp(83βJ) + 1 693 596 834exp(79βJ) + 5 582 009 274exp(75βJ) + 17 798 416 274exp(71βJ) + 54 823 098 984exp(67βJ) + 162 901 158 938exp(63βJ) + 466 124 104 712exp(59βJ) + 1 281 950 329 620exp(55βJ) + 3 381 468 336 320exp(51βJ) + 8 534 700 516 704exp(47βJ) + 20 558 823 116 544exp(43βJ) + 47 130 354 080 000exp(39βJ) + 102 502 065 432 576exp(35βJ) + 210 758 700 341 248exp(31βJ) + 408 115 654 279 168exp(27βJ) + 741 060 633 092 096exp(23βJ) + 1 255 720 425 046 016exp(19βJ) + 1 974 784 974 782 464exp(15βJ) + 2 864 301 246 447 616exp(11βJ) + 3 804 216 148 230 144exp(7βJ) + 4 588 063 201 689 600exp(3βJ) + 4 975 636 328 218 624exp(− 1βJ) + 4 795 773 478 502 400exp(− 5βJ) + 4 051 043 946 856 448exp(− 9βJ) + 2 948 121 001 787 392exp(− 13βJ) + 1 809 714 791 284 736exp(− 17βJ) + 912 536 471 986 064exp(− 21βJ) + 365 453 279 170 560exp(− 25βJ) + 111 283 316 092 160exp(− 29βJ) + 24 309 178 272 608exp(− 33βJ) + 3 503 944 500 290exp(− 37βJ) + 289 900 567 622exp(− 41βJ) + 10 032 960 838exp(− 45βJ)
---	---

tems on the equilateral wedges of the triangular lattice, with $b=3,4,\dots,15$ spins on a side. A selection ($b=9,10$) of obtained results is shown in Table II. In Fig. 3 we depict the results for $b=4,5,\dots,15$. The asymmetric form of the entropy curves in Fig. 3 corresponds to the intrinsic difference in the behavior of ferromagnetic and antiferromagnetic systems on the triangular lattice. This difference stems from the topological frustration of the antiferromagnetic system at low temperatures. The intercepts of the entropy curves with the right vertical axis (cf. Fig. 3) should be associated with the residual entropies in zero field of the finite Ising antiferromagnets on the triangular lattice. The comparison of the values that correspond to the mentioned intercepts with the exact residual entropy calculated by Wannier¹⁴ for the infinite system, is presented in Fig. 4. Hence, we can see that the results obtained for small fully finite systems converge rather well to the result found¹⁴ for the infinite system. A similar observation was recently made in the case of residual entropies of the 2D Ising antiferromagnet in the maximum critical field.¹⁵

We now proceed to study the specific heat of the 2D Ising systems in a zero field. It is a straightforward task to express any higher derivative of the partition function in terms of the degeneracies $\mathcal{D}_k^{(n)}$ defined by Eqs. (2). By differentiating (2a) twice with respect to temperature we obtain the expression for the specific heat

$$C^{(n)} = \frac{1}{k_B T^2} \left[\frac{Z_2^{(n)}}{Z^{(n)}} - \left[\frac{Z_1^{(n)}}{Z^{(n)}} \right]^2 \right], \quad (21a)$$

with

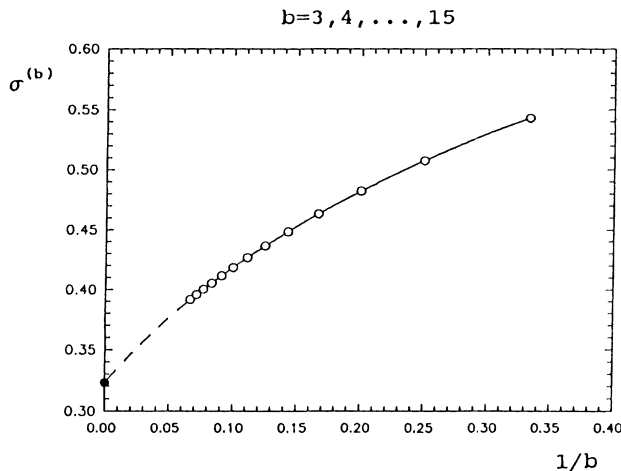


FIG. 4. Convergence of the zero-field residual entropies of the finite Ising antiferromagnets on the equilateral wedges of the triangular lattice with $b=3,4,\dots,15$ spins on a side (open circles), towards the exact value (Ref. 14) for the infinite system (solid circle). The data points (open circles) are derived from the intercepts of the curves depicted in Fig. 3 with the corresponding right vertical axes. The solid and the dashed lines serve as guides to the eye.

$$Z_1^{(n)} = \sum_{k=0}^{N_b^{(n)}} \mathcal{D}_k^{(n)} E_k^{(n)} e^{-\beta E_k^{(n)}}, \quad (21b)$$

and

$$Z_2^{(n)} = \sum_{k=0}^{N_b^{(n)}} \mathcal{D}_k^{(n)} (E_k^{(n)})^2 e^{-\beta E_k^{(n)}}. \quad (21c)$$

Using previously calculated degeneracies $\mathcal{D}_k^{(n)}$ to evaluate (21b) and (21c), for the square and triangular lattice, we have obtained the relevant specific heats from (21a). The corresponding curves are shown in Figs. 5. Here it should be stressed that, since within the presented approach we do not perform any *numerical* differentiation, the specific heats can be calculated with any preset accuracy.

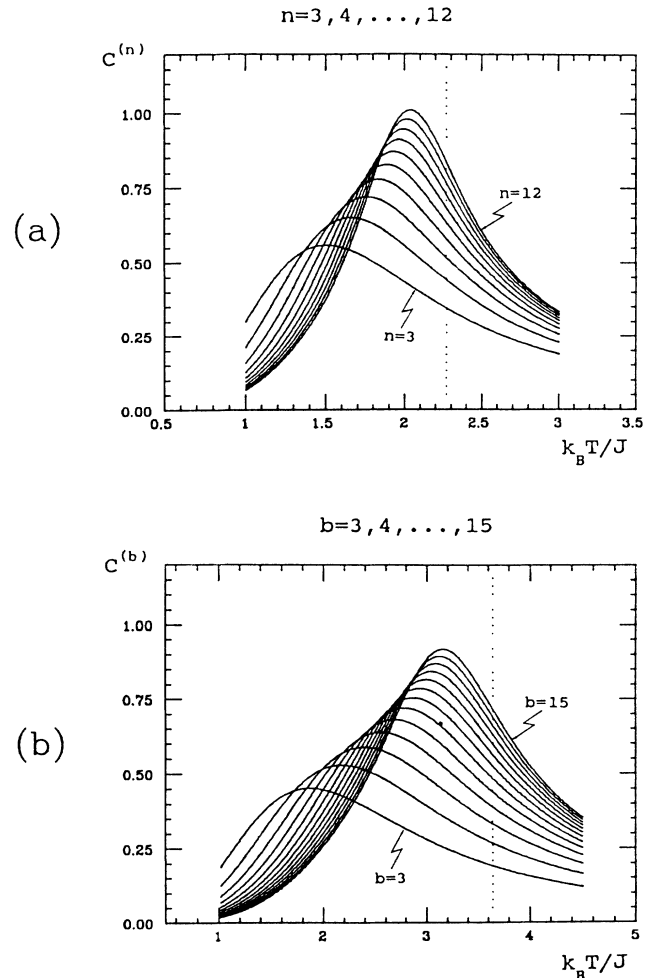


FIG. 5. The specific heat for fully finite lattices with free boundaries for: (a) the square lattice with $n \times n$ spins ($n=3,4,\dots,12$) and (b) equilateral wedges of the triangular lattice with $b=3,4,\dots,15$ spins on a side. The dashed vertical lines represent the critical temperatures of the corresponding infinite systems. The drawn curves are exact, in the sense that they do not represent a table of numerical data, but stem from the exact expression (21).

Results obtained for finite-size systems have been generally correlated to the description of the critical behavior of the infinite systems by the finite-size-scaling method.^{12,13} One of the most fascinating predictions of this method is the data collapsing of scaled thermodynamic response functions. This prediction has been checked using data obtained by the Monte Carlo calculations,^{10,11,16} and a fairly good confirmation has been obtained. The systems we have studied here are much smaller than the systems used to check the finite-size data-collapsing prediction. Nevertheless, it turns out that our data do support this prediction. In Fig. 6 we present the data from Fig. 5 in the form which should render data-collapsing according to the finite-size-scaling

theory prediction.¹³ We can see that although there is no total data collapsing, the curves for increasing system sizes display a strong merging tendency. In fact, the merging of the scaled specific heats that can be observed in Fig. 6 is the manifestation of the data collapsing. This data collapsing is by no means worse than the data collapsing provided by the Monte Carlo simulations for much larger systems (cf. Fig. 19 of Ref. 11). Thus the observable deviation from a total data collapsing in the Monte Carlo approach should not be ascribed primarily to the smallness of the systems studied, but rather to the intrinsic statistical error of the method used. In other words, it follows from our exact calculations that in the case of approximate studies of finite-size systems it is more important to reduce the error pertinent to the method applied, then to increase the system size.

IV. CASE $d=2$, $H \neq 0$

In this section we generalize the method of calculating and representing the DOS functions, elaborated in the first part of the paper, to the case of nonzero magnetic field ($H \neq 0$). The energy levels are now characterized by both the number of unsatisfied bonds k ($0 \leq k \leq N_b^{(m)}$) and the number l ($0 \leq l \leq N_s^{(m)}$) of spins antiparallel to the field, where $N_s^{(m)} = n \cdot m$ is the total number of spins. The corresponding partition function is given by the following analog of (2a)

$$Z^{(m)} = e^{\beta(|J|N_b^{(m)} + HN_s^{(m)})} \sum_{k=0}^{N_b^{(m)}} \sum_{l=0}^{N_s^{(m)}} Q_{kl}^{(m)} e^{-2\beta(k|J| + lH)}, \quad (22a)$$

whereas the energy levels are

$$E_{kl}^{(m)} = |J|(-N_b^{(m)} + 2k) + H(-N_s^{(m)} + 2l), \quad (22b)$$

with

$$k = 0, 1, \dots, N_b^{(m)} \quad \text{and} \quad l = 0, 1, \dots, N_s^{(m)}.$$

The degeneracies $Q_{kl}^{(m)}$, in addition to the analog of (2c)

$$\sum_{k=0}^{N_b^{(m)}} \sum_{l=0}^{N_s^{(m)}} Q_{kl}^{(m)} = 2^{nm}, \quad (22c)$$

satisfy

$$D_k^{(m)} = \sum_{l=0}^{N_s^{(m)}} Q_{kl}^{(m)}. \quad (22d)$$

For the partial partition functions we now have

$$Z^{(m)}(\gamma) = e^{\beta(|J|N_b^{(m)} + HN_s^{(m)})} \sum_{k=0}^{N_b^{(m)}} \sum_{l=0}^{N_s^{(m)}} Q_{kl}^{(m)}(\gamma) e^{-2\beta(k|J| + lH)}, \quad (23)$$

At this point we follow the algorithm behind formula (1b) and first find the energy levels of the added $(m+1)$ th chain

$$E(\gamma') = |J|[-(n-1) + 2l_{\gamma'}] + H(-n + 2s_{\gamma'}), \quad (24a)$$

and the energy levels of the interaction between the added chain and the rest of the system

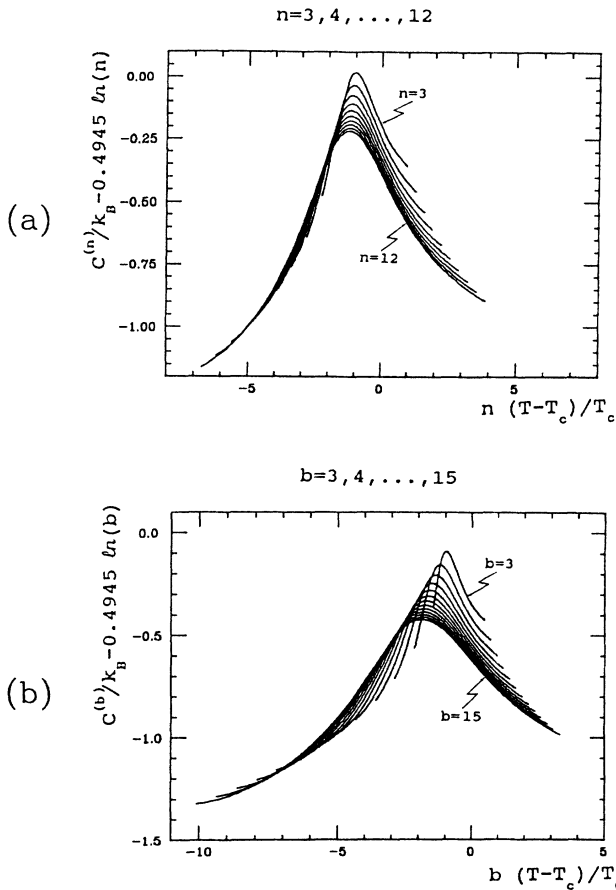


FIG. 6. The specific-heat data from Fig. 5 presented in the form which should render data collapsing according to the finite-size-scaling theory prediction (Ref. 13). Although there is no total data collapsing, there is a surprisingly strong merging tendency of the curves with increasing system size, both in the square lattice (a) and the triangular lattice (b) case. Thus, one should observe that in both cases the last few curves almost coincide. Furthermore, even if one considers all presented curves, the separation between them is no greater than the scattering of analogous data obtained by the Monte Carlo technique (Ref. 10) for much larger systems.

$$E_{\text{int}}(\gamma, \gamma') = |J|(-n + 2j_{\gamma, \gamma'}), \quad (24b) \quad \text{and}$$

$$j_{\gamma, \gamma'} = 0, 1, \dots, n.$$

where

$$l_{\gamma'} = 0, 1, \dots, n-1; \quad s_{\gamma'} = 0, 1, \dots, n$$

Inserting (22b), (23), and (24) into (1b), we find the recursion relation for calculating the DOS functions

$$Q_{k', l'}^{(m+1)}(\gamma') = \sum_{\gamma=1}^{2^n} \sum_{k=0}^{N_b^{(m)}} \sum_{l=0}^{N_s^{(m)}} Q_{kl}^{(m)}(\gamma) \delta(k' - k - l_{\gamma'}) \delta(l' - l - s_{\gamma'}) \quad (25)$$

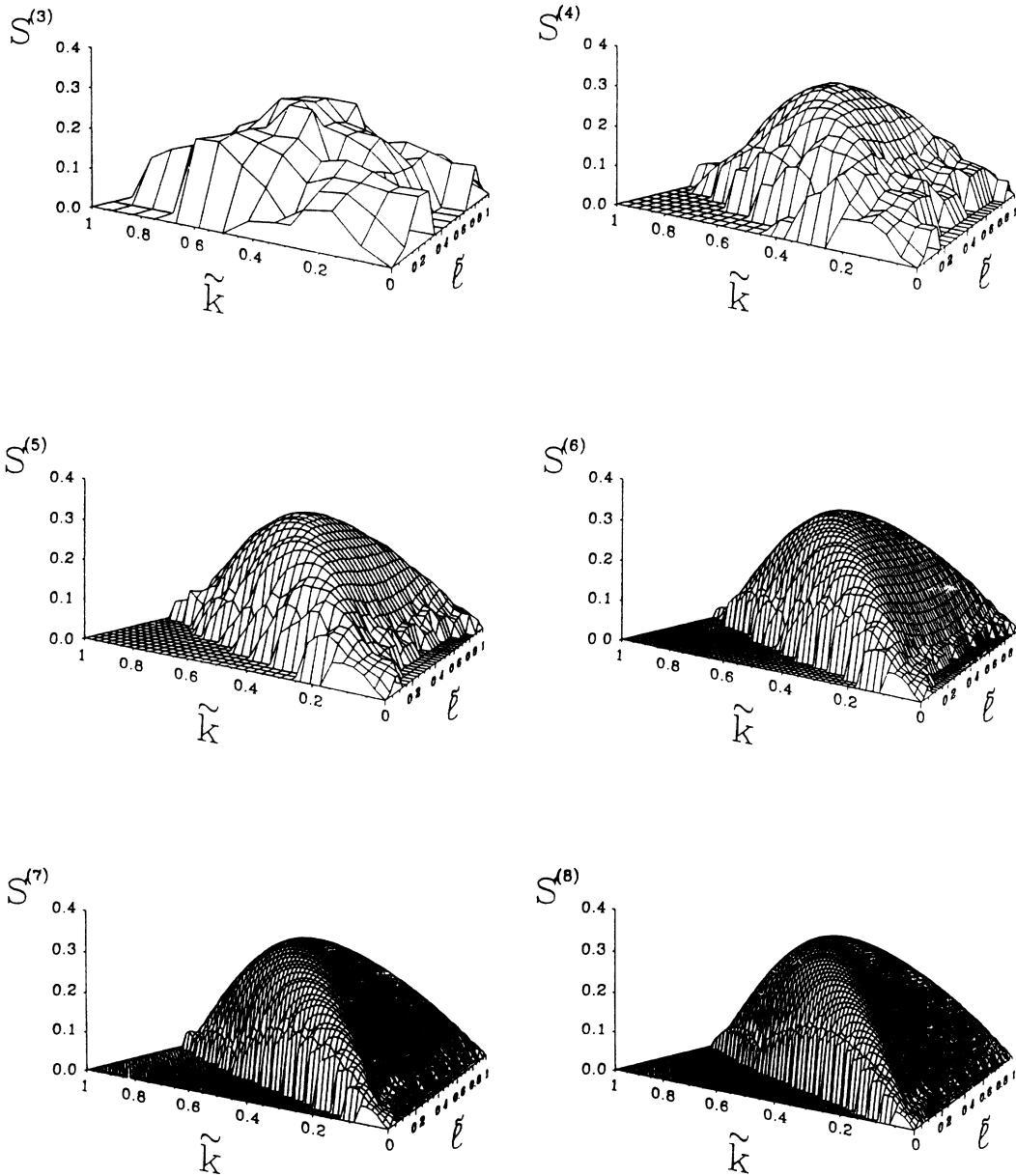


FIG. 7. The first exact solution of the fully finite square Ising model, with free boundaries, in a magnetic field, presented through the scaled DOS functions $S^{(n)}(k, l)$ vs variables $\tilde{k} = k/N_b$ and $\tilde{l} = l/N_s$, for $n = 3, 4, 5, 6, 7, 8$. One should notice the unexpectedly regular shape of the DOS surfaces for systems with already 6×6 spins. In addition, one should observe that these surfaces are independent of the specific values of T , H , and J .

with

$$Q_{kl}^{(m)} = \sum_{\gamma=0}^{2^n} Q_{kl}^{(m)}(\gamma). \quad (26)$$

Here we should make the same comment we have made in discussing implementation of formula (7). Namely, for a given combination of γ and γ' , it is not necessary to scan all possible combinations of k, k', l and l' in order to see which of them give a nonzero contribution in (25). Instead, for each particular set of γ, γ', k , and l , the Kronecker δ functions in (25) should be used to find those values of k' and l' for which the degeneracy $Q_{k',l'}^{(m+1)}(\gamma')$ is increased by the term $Q_{kl}^{(m)}(\gamma)$. In this way the total number of necessary operations is reduced roughly from

$$N_b^{(m)} N_b^{(m+1)} N_s^{(m)} N_s^{(m+1)} 2^{2n} \approx (nm)^4 2^{1n+2}$$

to

$$N_b^{(m)} N_s^{(m)} 2^{2n} \approx (nm)^2 2^{2n+1},$$

which is a larger reduction than in the $H=0$ case. Compared to the numerical TM approach and the $H=0$ case (elaborated in Sec. IIa), both the necessary CPU time and memory requirements are now increased. However, a single computer run is sufficient to generate all necessary information for all temperatures, *all fields* and all possible values of the interaction strength, instead of the tabular information provided by the numerical TM approach.

We have performed specific calculations for the square lattice Ising model with $n \times n$ spins, $n=2, 3, \dots, 8$. In order to display the obtained results in a suitable form, we rewrite (22a) in the form analogous to (16)

$$Z^{(n)} = \sum_{k=0}^{N_b^{(n)}} \sum_{l=0}^{N_s^{(n)}} \exp[-\beta(E_{kl}^{(n)} - k_B T \ln Q_{kl}^{(n)})]. \quad (27)$$

For depicting the DOS functions $Q_{kl}^{(n)}$, we introduce the entropy of the energy level $E_{kl}^{(n)}$

$$S_{kl}^{(n)} = \frac{\ln Q_{kl}^{(n)}}{N_b^{(n)}}.$$

In the $H=0$ case, we have analyzed the relevant entropy as a function of the variable $\bar{k} \equiv k/N_b^{(n)}$. Since in the case $H \neq 0$ the energy levels are classified by two integers l and k , it is convenient now to represent the entropy as a function of the two variables $\bar{k} = k/N_b^{(n)}$ and $\bar{l} = l/N_s^{(n)}$. Both variables have values in the interval $[0, 1]$, and each pair of values corresponds to a definite energy level [cf. Eq. (22b)]. Thus the DOS functions appear to be surfaces above the (\bar{k}, \bar{l}) plane.

Our results for the DOS functions of systems of different sizes are shown in Fig. 7 (a table of these results presented in the form of Table I. would be approximately twenty times larger for systems of same sizes). Compared with Fig. 2 we can see that now the convergence of the DOS functions is manifested through rapid smoothing of the surfaces with increasing size of the system (measured by n). A definite shape of the DOS function surface

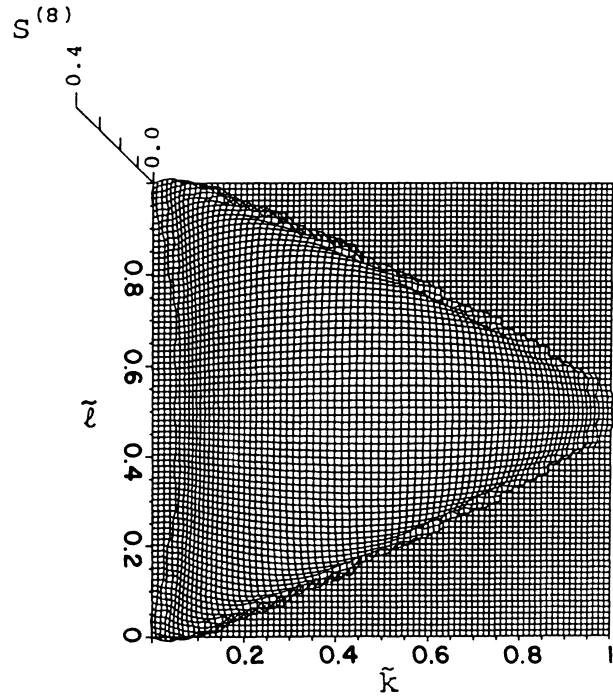


FIG. 8. The DOS function surface from Fig. 7 (in the case $n=8$) depicted in a differently positioned system of coordinates to display the symmetry with respect to the $\bar{l}=0.5$ plane.

(versus variables \bar{k} and \bar{l}) one would expect in the limit $n \rightarrow \infty$, and knowing this shape would be equivalent to knowing the exact solution of the square Ising model in a field. What comes as a surprise from Fig. 7 is the fact that already such small systems as 7×7 and 8×8 disclose a quite definite shape of the DOS function surface. In fact, it is hard to believe that the observed shape would

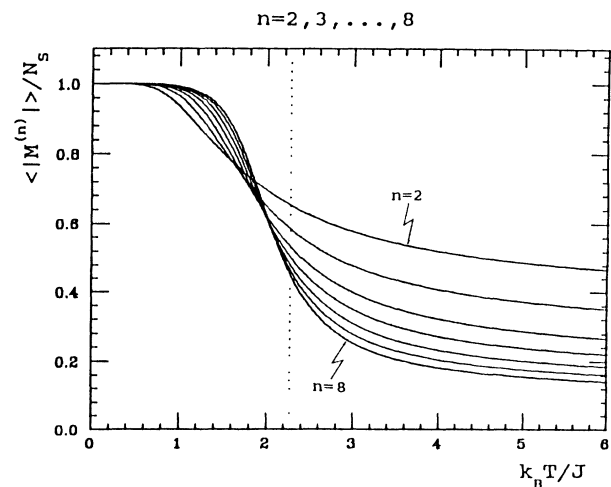


FIG. 9. The exact magnetization of the square lattice Ising model in zero field with $n \times n$ spins ($n=2, 3, \dots, 8$), calculated according to the formula (28). The dotted vertical line corresponds to the critical temperature of the infinite system.

substantially change with further increasing of n . To provide a more complete display of the DOS surface we present in Fig. 8 our results for the 8×8 Ising model in a differently positioned system of coordinates.

Having concrete results for $H \neq 0$, we are going to study the corresponding magnetization and susceptibility. For a system of size $n \times n$ we adopt the standard definition¹¹ of magnetization (order parameter)

$$\langle |M| \rangle = \frac{\sum_{k=0}^{N_b^{(n)}} \sum_{l=0}^{N_s^{(n)}} Q_{kl}^{(n)} |N_s^{(n)} - 2l| e^{-\beta E_{kl}^{(n)}}}{Z^{(n)}}, \quad (28)$$

and susceptibility

$$\chi = \beta (\langle M^2 \rangle - \langle |M| \rangle^2), \quad (29)$$

where

$$\langle M^2 \rangle = \frac{\sum_{k=0}^{N_b^{(n)}} \sum_{l=0}^{N_s^{(n)}} Q_{kl}^{(n)} (N_s^{(n)} - 2l)^2 e^{-\beta E_{kl}^{(n)}}}{Z^{(n)}}. \quad (30)$$

Using our data for $Q_{kl}^{(n)}$ and $E_{kl}^{(n)}$ we have calculated magnetization and susceptibility according to the preceding formulas. The obtained results are presented in Figs. 9 and 10. In Fig. 11 we present the data from Fig. 10 in the form expected to exhibit data collapsing according to the finite-size-scaling theory.^{11,13} Similarly to the case of specific heat (cf. Fig. 6), there is no total data collapsing for all n but the curves for $n=7$ and $n=8$, in Fig. 11, *practically coincide*. Furthermore, comparing our Fig. 11 with Fig. 18 of Ref. 11 which was obtained for much larger systems using Monte Carlo method, one can notice a similar deviation from total data collapsing. Thus one can infer the same conclusion as in the specific-heat case, that is to say in checking and applying the finite-size-

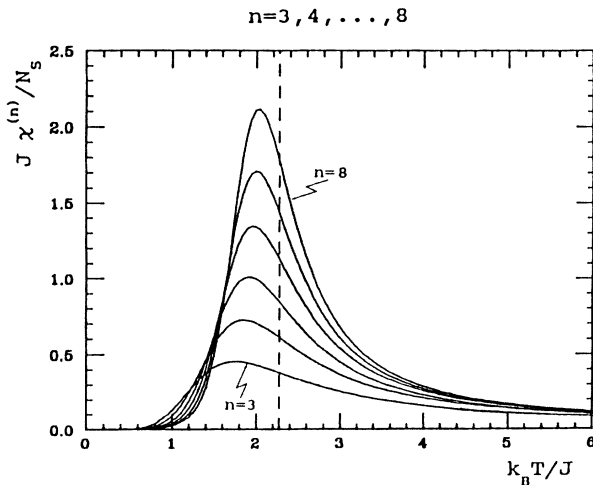


FIG. 10. The exact zero-field susceptibility of the fully finite square lattice Ising model, with $n \times n$ spins ($n = 3, 4, \dots, 8$), calculated according to the formula (29). The dashed line corresponds to the critical temperature of the infinite system.

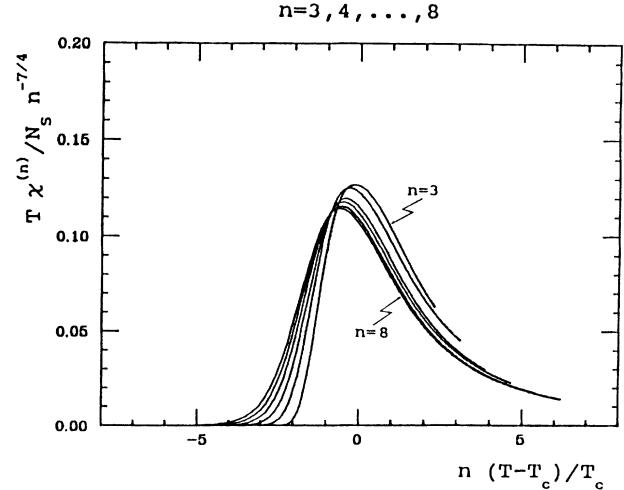


FIG. 11. The susceptibility data from Fig. 10 in the form that should render data collapsing according to the finite-size-scaling theory prediction (Refs. 11 and 13). It is surprising that data for such small systems, when calculated exactly, exhibit such a strong merging tendency even in the critical region pertinent to the infinite system.

scaling predictions via approximate methods it is more important to improve the accuracy than to increase the size of the systems studied.

V. CONCLUSION

In this paper we use the transfer matrix (TM) method⁶ to calculate the density-of-states functions of fully finite Ising model systems with free boundaries. As a result of this approach expressions for the partition function for systems up to 12×12 spins are obtained. Although the applicability of this approach is in general restricted by the performance of present-day computers to studying relatively small systems, there are several advantages compared to strictly numerical and approximate methods. One advantage over strictly numerical methods is that the study of thermodynamic properties is facilitated by the fact that all higher derivatives of the partition function are obtained as analytic functions of T and H . Thus, only one computer run is sufficient to obtain necessary information for all temperatures, all fields and all values of the interaction strength, compared to the numerical TM approach⁷ which yields results in a tabular form for discrete preset values of T and H .

An interesting finding achieved via the TM approach is the fact that the DOS functions for systems of increasing sizes display in each particular case a rapid convergence towards their thermodynamic limiting values. This convergence has been first demonstrated in the case of the simple Ising chain in zero field (cf. Fig. 1), but it appears to be more rapid in the case of the two-dimensional Ising model (cf. Figs. 2 and 3). In the $H=0$ square lattice case we have calculated the DOS functions for $n \times n$ systems with $n = 3, 4, \dots, 12$. Expressions for the partition function for $n = 4, 5, 6$ are given in Table I, while the scaled DOS functions are depicted in Fig. 2. The rapid conver-

gence is manifested through merging of the curves for $n > 3$ into a bundle whose elements are hardly distinguishable from each other. In the $H=0$ triangular lattice case we have calculated the DOS functions for Ising systems on equilateral wedges of the triangular lattice, with $b=2, 3, \dots, 15$ spins on a side. A selection of expressions for the partition function is given in Table II, while in Fig. 3 we depict the scaled DOS functions, which again exhibit rapid convergence. In the $H \neq 0$ case we have calculated the DOS functions for $n \times n$ Ising systems on the square lattice with $n=2, 3, \dots, 8$. In Fig. 7 we depict the scaled DOS functions which are represented as surfaces over two independent variables \bar{k} and \bar{l} . The convergence is now manifested through rapid smoothing of the surfaces with increasing size of the system.

One of the most fascinating features related to the discovered convergence of the DOS functions is the fact that it is observable already for small systems studied in this paper. This allows one to learn certain properties of the infinite systems. For instance, from the bundle of the scaled DOS function curves (see, e.g., Fig. 2 and the related text) one can learn those energy levels that give the dominant contribution to the partition function for each given temperature and field. Besides, in the case of the triangular lattice, the intercepts of the scaled DOS function curves with the right vertical axis (cf. Figs. 3 and 4) can be straightforwardly related to the residual entropy of the infinitely large Ising antiferromagnet¹⁴ in zero field. Furthermore, one may argue that the observed DOS functions convergence is a precursor of the data collapsing of the response functions predicted by the finite size scaling theory.¹³ Indeed, starting with our data for the DOS functions we have also calculated the specific heats for both the square and the triangular lattice, the results being shown in Fig. 5. In Fig. 6 we present the same results in the form which should exhibit data collapsing ac-

ording to the finite-size-scaling theory prediction.¹³ We can see that there is no total data collapsing, but the curves for increasing system sizes display a strong merging tendency. The fact that this merging is comparable to data collapsing obtained¹¹ for much larger systems by Monte Carlo simulations, implies that in the approximate studies of finite size systems it is more important to reduce the error pertinent to the method applied than to increase the system size. A similar conclusion can be drawn from our results for zero-field susceptibility presented in Figs. 10 and 11.

At the end, it should be emphasized that additional new results can be easily achieved by applying the presented approach using more powerful computers which are available nowadays. This approach of calculating and analyzing the DOS functions can be also easily extended to other situations, such as three-dimensional Ising systems, impurities, random fields, or other models.

ACKNOWLEDGMENTS

One of the authors (B.S.) is grateful to the Center for Polymer Studies and Department of Physics of Boston University for the the kind hospitality extended to him during a leave of absence from his native institute. We also wish to thank Professor K. Binder for helpful correspondence and generous constructive criticism. Stimulating discussions with Professor H. W. Capel are gratefully acknowledged. This work was supported in part by the Yugoslav-U.S.A. Joint Scientific Board under Project No JF900, National Science Foundation (NSF), by the Yugoslav Federal Science Funds under Project No. P-26, and by the Serbian Science Foundation under Project No. 1.27.

¹L. Onsager, Phys. Rev. **6**, 117 (1944).

²B. Kaufman, Phys. Rev. **76**, 1232 (1949).

³A. E. Ferdinand and M. E. Fisher, Phys. Rev. **185**, 832 (1969).

⁴S. Ono, Y. Karaki, M. Suzuki, and C. Kawabata, J. Phys. Soc. Jpn. **25**, 54 (1968).

⁵M. Suzuki, C. Kawabata, S. Ono, Y. Karaki, and M. Ikeda, J. Phys. Soc. Jpn. **29**, 837 (1970).

⁶K. Binder, Physica **62**, 508 (1972).

⁷I. Morgenstern and K. Binder, Phys. Rev. B **22**, 288 (1980).

⁸We have used the IBM 3090 mainframe computer at the Boston University. In the case 8×8 ($H \neq 0$) the used CPU time was approximately 2 minutes, while in the case 12×12 ($H=0$) the used CPU time was approximately 30 minutes. The main computer constraint in these calculations was the available memory (11 Mbytes) rather than CPU time.

⁹A. Ferrenberg and H. Swendsen, Phys. Rev. Lett. **61**, 2635 (1988).

¹⁰D. P. Landau, in *Magnetism and Magnetic Materials (San Francisco, 1974)*, Proceedings of the 20th Annual Conference on Magnetism and Magnetic Material, AIP Conf. Proc. No. **24**, edited by C. D. Graham, G. H. Lander, and J. J. Rhyne (AIP, New York, 1975).

¹¹D. P. Landau, Phys. Rev. B **13**, 2997 (1976).

¹²M. E. Fisher, in *Critical Phenomena*, edited by M. S. Green (Academic, New York, 1971).

¹³M. N. Barber, in *Phase Transitions and Critical Phenomena*, edited by C. Domb and J. L. Lebowitz (Academic, New York, 1983), Vol. VIII.

¹⁴G. H. Wannier, Phys. Rev. **79**, 357 (1950); G. H. Wannier, Phys. Rev. B **7**, 5017 (1973).a

¹⁵S. Milošević, B. Stošić, and T. Stošić, Physica A **157**, 899 (1989).

¹⁶K. Binder, Ferroelectrics **73**, 43 (1987).